Supplemental Information

Direct transcriptional regulation of Nrp2 by COUP-TFII modulates multiple steps in murine lymphatic vessel development

Fu-Jung Lin, Xinpu Chen, Jun Qin, Young-Kwon Hong, Ming-Jer Tsai, and Sophia Y. Tsai

Supplemental Experimental Procedures

Mouse Strain and Histology

The *SM22αCre* mouse strain has been described previously (1). *COUP-TFII*$^{flox/flox}$ mice were crossed with *SM22αCre; COUP-TFII*$^{flox/+}$ to generate *SM22αCre; COUP-TFII*$^{flox/flox}$ embryos. The mouse strain was maintained in a mixed genetic background (129/Sv x C57BL/6) and received standard rodent chow.

Histological Analysis and Immunohistochemistry

Mouse tissues were fixed with 4% paraformaldehyde (PFA), dehydrated, and embedded in paraffin. For histological analysis, sections (7 μm) were stained with hematoxylin and eosin (H&E). For immunohistochemistry, deparaffinized sections after antigen retrieval were blocked with 5% donkey serum and a biotin-blocking system (DakoCytomation). The following primary antibodies were used for immunostaining of mouse tissues: monoclonal mouse anti-human COUP-TFII (Perseus Proteomics), polyclonal goat anti-mouse EphB4, polyclonal goat anti-mouse VEGFR3, polyclonal goat anti-rat Neuropilin-1, polyclonal goat anti-rat Neuropilin-2, polyclonal goat anti-mouse Endoglin (R&D Systems), monoclonal anti-rabbit VEGFR2 (Cell Signaling Technology), rabbit anti-

Prox1, rabbit anti-mouse LYVE1 (AngioBio), hamster anti-mouse Podoplanin (clone 8.1.1; Hybridoma Bank, University of Iowa), rabbit anti-laminin (DakoCytomation), rabbit anti-collagen IV (Abcam), mouse anti-human Ki67 (BD Biosciences), and monoclonal rat anti-mouse CD31 (PECAM) (clone MEC 13.3; BD Biosciences). Sections were washed with PBST buffer and incubated with biotinylated secondary antibodies (Jackson ImmunoResearch). Signal detection was carried out with the Avidin-Biotin Complex kit (Vector Laboratories) or Tyramide Signal Amplification system (TSA, Invitrogen). Peroxidase activity was visualized with 3,3'-diaminobenzidine (DAB, Vector Laboratories). Nuclear staining was carried out with 4,6-diamidino-2-phenylindole (DAPI; Sigma), and sections were mounted with Vectashield mounting medium (Vector Laboratories) prior to imaging. Images were captured with a Zeiss Axiophoto fluorescence microscope.

For whole-mount immunofluorescence staining, embryonic back skins or dorsal segments of adult mouse ears were dissected and fixed with 4% PFA overnight at 4ºC. Primary antibodies in a blocking solution (2% nonfat skim milk in phosphate buffered saline (PBS) with 0.5% Triton X-100) were added and incubated overnight at 4ºC. Tissues were washed for 5 h and incubated with biotinylated secondary antibodies (Jackson ImmunoResearch) for 1 h at room temperature. Signals were amplified with a TSA kit (Invitrogen). Specimens were imaged and analyzed using the Zeiss Axioplan 2 imaging microscope with MetaMorph software.

Western Blot Analysis

24 hours after transfection, LECs were lysed with 1X RIPA buffer containing 1X TBS, 1% Nonidet P-40, 0.5% sodium deoxycholate, 0.1% SDS, a protease inhibitor cocktail (Roche Applied Science), and a phosphatase inhibitor cocktail (Sigma) for 30 minutes on ice. After centrifugation for 15 minutes, the supernatant was collected, and protein content of the samples was analyzed according to the Bradford method. Proteins were loaded onto SDS-polyacrylamide gels and blotted onto PVDF membranes (Bio-Rad Laboratories). Western blots were performed using antibodies directed against COUP-TFII (Perseus Proteomics), Neuropilin-2, and HRP-conjugated β-actin (Santa Cruz Biotechnology). Enhanced chemiluminescence was performed according to the manufacturer's instructions (Amershan Biosciences, UK).

FACS Analysis

Mouse lung EC isolation was carried out as described (2). Briefly, mice were anesthetized with avertin, perfused with PBS, intra-tracheally injected with 1 mL dispase (BD Biosciences) and 1mL 1% agarose. Lungs were isolated, minced, and treated with 2 mg/mL collagenase/dispase (Roche) and 10 ug/mL DNase (Sigma) in PBS at 37ºC for 45 minutes to produce a single-cell suspension. The tissue was then filtered through 100 μm and 40 μm cell strainers (BD Biosciences), and centrifuged at 2000 rpm, 5 minutes. Subsequently, cells were resuspended and labeled with a biotinylated anti-CD31 antibody (BD Biosciences) and anti-bitotin microbeads (Miltenyi Biotec). ECs were first separated from other components by using AutoMACS (Miltenyi Biotec), and then Fluorescence Activated Cell Sorting (FACS) was performed.

For EC isolation from mouse embryos, E14.5 mouse embryos were dissected and the embryonic liver was removed microscopically. The embryos were then minced into pieces and digested with 2 mg/mL collagenase/dispase (Roche) and 25 ug/mL DNase (Sigma) in PBS at 37ºC for 45 minutes. Embryonic ECs were isolated by the method described above.

In Vitro Proliferation Assay

Human primary LECs were transfected with scrambled or *COUP-TFII* siRNA for 48 hours. SiRNA-treated LECs were re-plated and incubated at 2.4 x10^4 cells per well in 48-well plates coated with fibronectin (10 ng/mL), deprived of FBS for 12 hours, followed by stimulation with or without 60 ng/mL of VEGF-C in a cultured medium for 48 hours or 72 hours. Then cells were trypsinized at the indicated time points and cell numbers were counted using a hemocytometer.

Construction of Luciferase Plasmid and Luciferase Assay

The mouse *Nrp2* promoter fragment encompassing nucleotides -2885 to +920 was generated by PCR with the forward primer 5'-CCAAGAGCTCGCTGAATCCAGCTCC ACAAACTCC-3' (*SacI* site underlined) and the reverse primer 5'-AAAACTCGAGTTT TGACAGAGAGGCTCT CTCCGG-3' (*XhoI* site underlined), using the Expand High Fidelity system (Roche), according to the manufacturer's instructions. BAC clone RP24-163014 (CHORI) was used as a template and the PCR product was digested with *SacI* and *XhoI* and ligated into the *SacI/XhoI* sites of the pGL2 basic luciferase reporter vector (Promega). The construct was verified by sequencing. HEK293T cells (2 x 10^5 per well)

were cotransfected with 150 ng of pGL2-Nrp2 or pGL2 basic vectors in the presence of an empty control vector or a COUP-TFII expressing vector using Lipofectamine 2000 (Invitrogen). Cells were cotransfected with 100 ng of β-gal plasmid to account for variation in transfection efficiencies. Luciferase activity was measured using the luciferase assay system following the manufacturer's protocol (Promega). Luciferase activity was normalized to β-gal activity.

Supplemental Table 1. The target sequences for human siRNA

	Sequences
hCOUP-TFII single 1	GUAUUAUAAUUGUUGAUAU
hCOUP-TFII single 2	CUUAGUUCUUGAAUUGUUA
hCOUP-TFII pooled	GUAUUAUAAUUGUUGAUAU CUUAGUUCUUGAAUUGUUA GUCGAGUCUUUGUGUGUUA GGAGGAACCACAUAUAACA
hProx1 pooled	UAUACAAGGUCAUCUGCAA GUUCUGAGCAGGAUGUUGA GGGCCAAACUCCUUACAAC GACGUAAAGUUCAACAGAU

Supplemental Table 2. The primer sequences for Q RT-PCR

Gene	Primer sequences	Size (bp)	References
hCOUP-TFII	F: GCCATAGTCCTGTTCACCTC R: CTGAGACTTTTCCTGCAAGC	79	(3)
hVEGFR3	F: CAAGGCCAACAACGGCAT R: TCGACGCTGATGAAGGGG	78	(4)
hProx1	F: CCCAGGACAGTTTATTGACCGA R: GGTTGTAAGGAGTTTGGCCCAT	120	This report
hPodoplanin	F: CGAAGATGATGTGGTGACTCCA R: CGATGCGAATGCCTGTTACA	104	This report
hNrp2	F: GGATGGCATTCCACATGTTG R: ACCAGGTAGTAACGCGCAGAG	153	(5)
hLYVE1	F: GCTTTCCATCCAGGTGTCAT R: AGCCTACAGGCCTCCTTAGC	102	This report
hNrp1	F: TTCAGGGCCATTTCTTTTTATC R: GGAACATTCAGGACCTCTCTTG	103	This report

hEphB4	F: CCATCAAAATGGGAAGATACGA R: CCAAGATTTTCTTCTGGTGTCC	135	This report
h18s RNA	F: TCCGATAACGAACGAGACTC R: CAG GGACTTAATCAACGCAA	81	(6)

Supplemental Table 3. The primer sequences for ChIP

Gene	Primer sequences
hNrp2	F: CTGACATCCACATGCTGCTC R: GAGTGTCTGTGCGGCTGA
hNrp2-neg	F: TGATTCGCTGTGTGTGTGTG R: CGAACATCTGGGGTAGGAGA
hFGFR3	F: GCTCACACCACAGGGTTCA R: GCAGGCCTGTGTTTGCATAG
hFGFR3-neg	F: CAGCCGCTTCTTTGTACCTC R: AATGACACGCACATTCAAGC

Supplemental References:

1. Holtwick, R., Gotthardt, M., Skryabin, B., Steinmetz, M., Potthast, R., Zetsche, B., Hammer, R.E., Herz, J., and Kuhn, M. 2002. Smooth muscle-selective deletion of guanylyl cyclase-A prevents the acute but not chronic effects of ANP on blood pressure. *Proc Natl Acad Sci U S A* 99:7142-7147.
2. Kim, C.F., Jackson, E.L., Woolfenden, A.E., Lawrence, S., Babar, I., Vogel, S., Crowley, D., Bronson, R.T., and Jacks, T. 2005. Identification of bronchioalveolar stem cells in normal lung and lung cancer. *Cell* 121:823-835.
3. Xu, X.C., Lee, J.J., Wu, T.T., Hoque, A., Ajani, J.A., and Lippman, S.M. 2005. Increased retinoic acid receptor-beta4 correlates in vivo with reduced retinoic acid receptor-beta2 in esophageal squamous cell carcinoma. *Cancer Epidemiol Biomarkers Prev* 14:826-829.

4. Li, J., Wang, E., Rinaldo, F., and Datta, K. 2005. Upregulation of VEGF-C by androgen depletion: the involvement of IGF-IR-FOXO pathway. *Oncogene* 24:5510-5520.

5. Curreli, S., Arany, Z., Gerardy-Schahn, R., Mann, D., and Stamatos, N.M. 2007. Polysialylated neuropilin-2 is expressed on the surface of human dendritic cells and modulates dendritic cell-T lymphocyte interactions. *J Biol Chem* 282:30346-30356.

6. Harmancey, R., Senard, J.M., Pathak, A., Desmoulin, F., Claparols, C., Rouet, P., and Smih, F. 2005. The vasoactive peptide adrenomedullin is secreted by adipocytes and inhibits lipolysis through NO-mediated beta-adrenergic agonist oxidation. *Faseb J* 19:1045-1047.

7. Shin, J.W., Min, M., Larrieu-Lahargue, F., Canron, X., Kunstfeld, R., Nguyen, L., Henderson, J.E., Bikfalvi, A., Detmar, M., and Hong, Y.K. 2006. Prox1 promotes lineage-specific expression of fibroblast growth factor (FGF) receptor-3 in lymphatic endothelium: a role for FGF signaling in lymphangiogenesis. *Mol Biol Cell* 17:576-584.

Supplemental Results

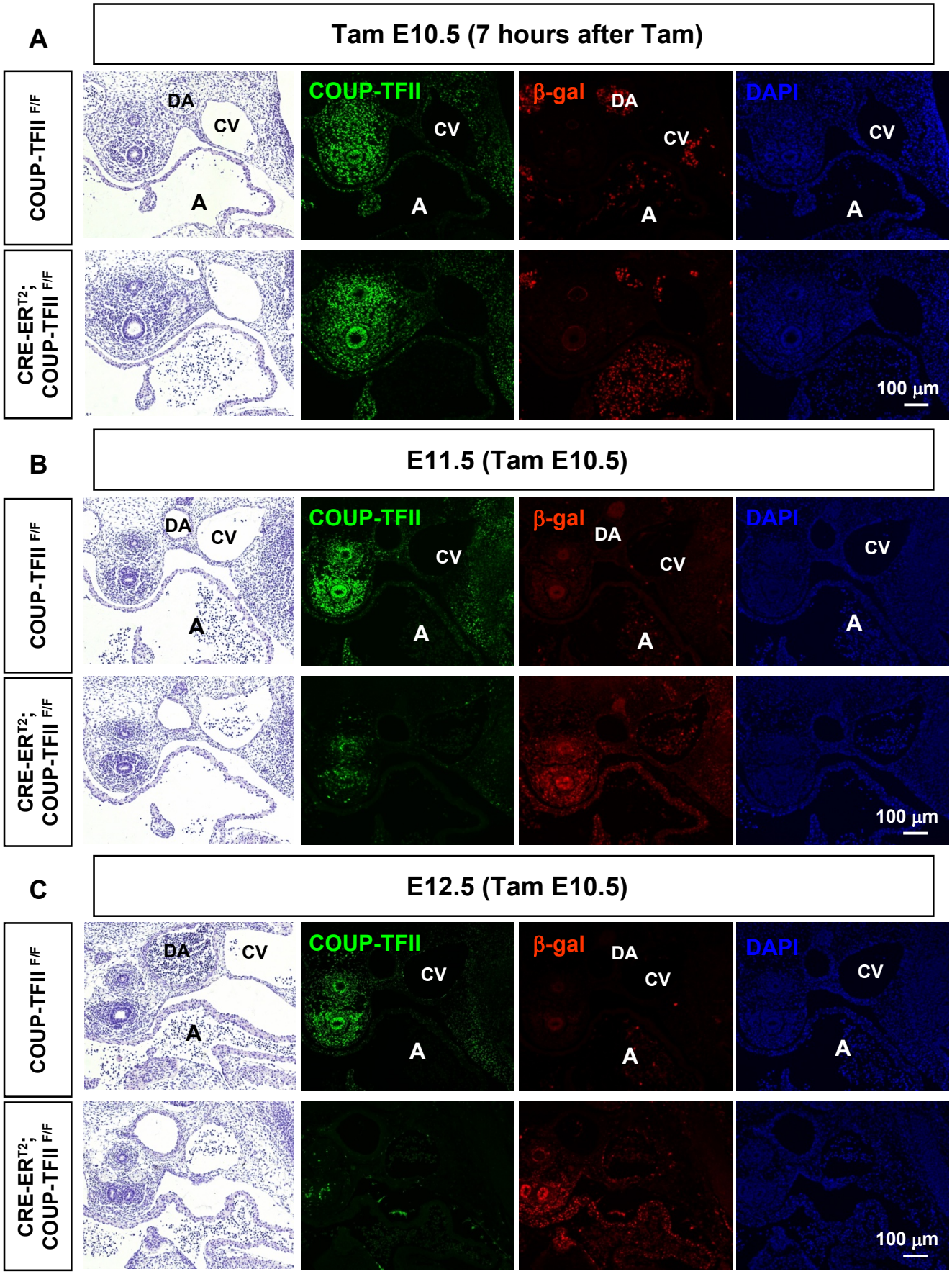

Supplementary Figure 1. Kinetics of *CRE-ER^{T2}* mediated *COUP-TFII* inactivation.
A single dosage of 3 mg Tam was delivered by intraperitoneal injection to pregnant dams at E10.5, and embryos were harvested at 7 hours (A), 1 day (B), and 2 days (C) after Tam treatment. H&E staining and immunofluorescence for COUP-TFII (green) and β-gal (red) were observed in transverse sections of control *COUP-TFII $^{F/F}$* and *CRE-ER^{T2}; COUP-TFII $^{F/F}$* embryos. Nuclei were counterstained with DAPI. Injection of Tam activates *CRE-ER^{T2}*, triggering *COUP-TFII* excision by recombination. Upon *Cre*-mediated recombination, the *Lac-Z* reporter inserted into the 5' untranslated region of *COUP-TFII* locus is activated. (A) Embryos exposed to Tam for 7 hours showed few or no β-gal^{+} cells. (B) One day after Tam administration *COUP-TFII* deletion and corresponding β-gal activation were observed in around 80% of cells (C) *COUP-TFII* deletion is almost complete 2 days post injection. A, atrium; CV, cardinal vein; DA, dorsal aorta. Scale bar, 100 μm.

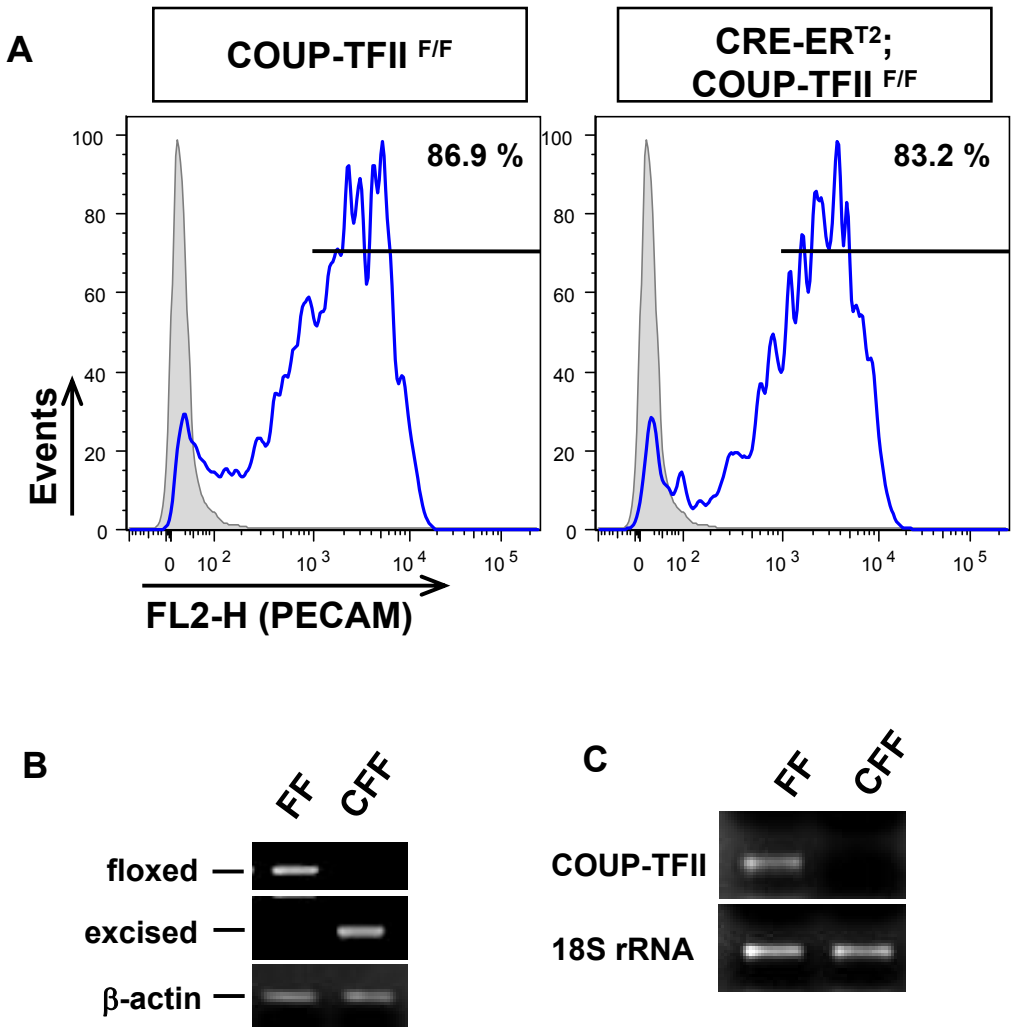

Supplemental Figure 2. Efficient inactivation of *COUP-TFII* in embryonic ECs.
(A) ECs were isolated from E14.5 *COUP-TFII* $^{F/F}$ (FF) controls and *CRE-ER*^{T2}*; COUP-TFII* $^{F/F}$ (CFF) embryos (administration of Tam at E11.5). Whole embryos were mechanically disrupted and enzymatically digested to create a single-cell suspension. Cells were labeled with PECAM antibodies. The endothelial content was enriched from less than 1% to more than 80% of the total tissue mass using magnetic cell sorting (MACS) separation. The selected fraction of cells was further analyzed by FACS. Gray histograms represent the isotype control. PECAM-gated ECs were sorted. (B) Genomic DNAs were isolated from sorted cells for PCR genotyping and allele excision analysis. β-actin was used as a loading control. (C) *COUP-TFII* expression in sorted ECs from *COUP-TFII* $^{F/F}$ and *CRE-ER*^{T2}*; COUP-TFII* $^{F/F}$ embryos were analyzed by semi-quantitative RT-PCR. 18S rRNA was used as a loading control.

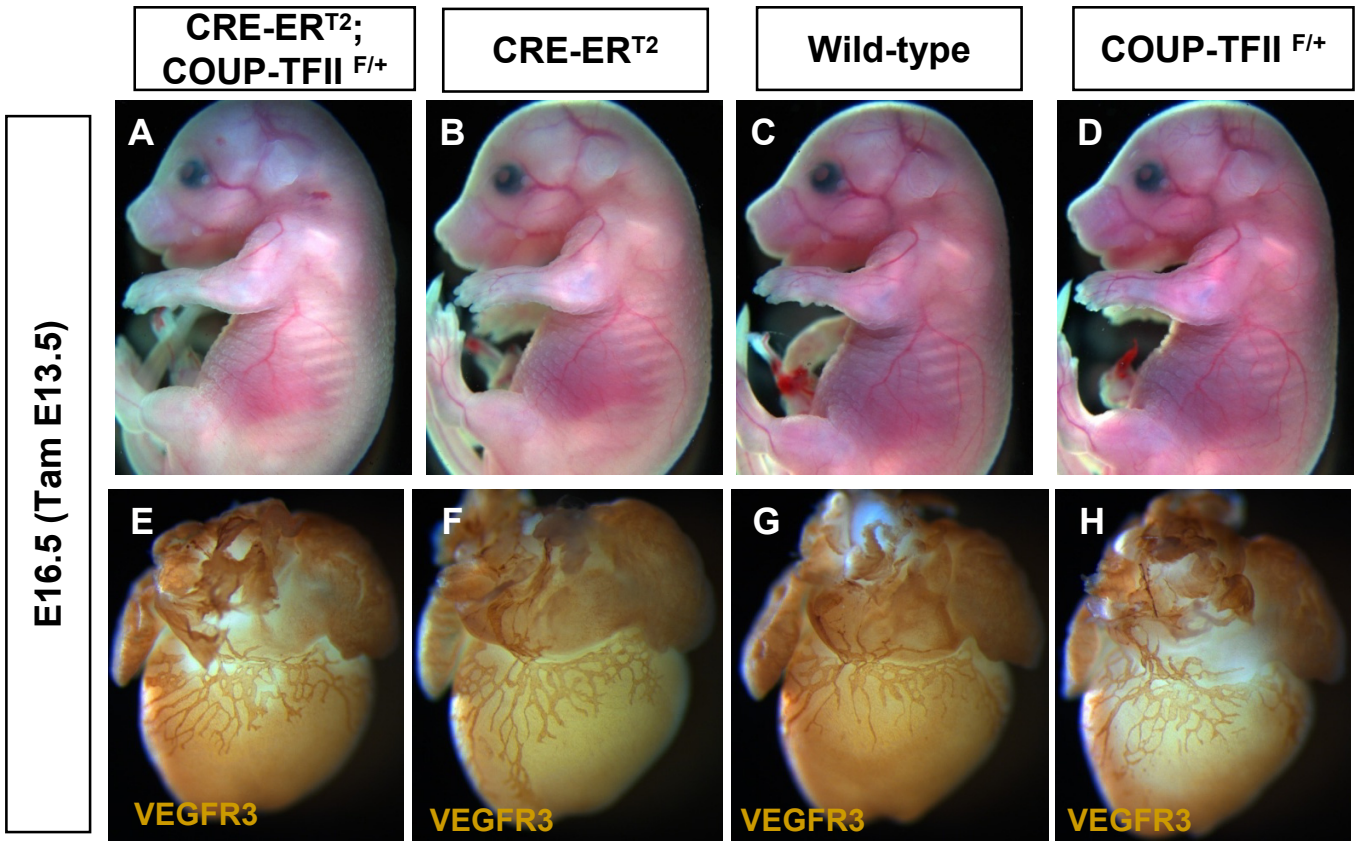

Supplementary Figure 3. Developmental defects observed in inducible *COUP-TFII* knockout mutants are due to ablation of *COUP-TFII*.
CRE-ER^{T2}; COUP-TFII $^{F/F}$ males were crossed to *COUP-TFII $^{F/+}$* females, and pregnant dams were injected with Tam at E13.5. Embryonic hearts were isolated at E16.5 and analyzed by whole mount VEGFR3 staining. (A-D) Gross appearance of *CRE-ER^{T2}; COUP-TFII $^{F/+}$* and *CRE-ER^{T2}* controls are indistinguishable from wild-type or *COUP-TFII $^{F/+}$* controls. (E-H) Whole mount VEGFR3 staining of E16.5 mouse hearts revealed similar cardiac lymphatic patterning *in CRE-ER^{T2}; COUP-TFII $^{F/+}$*, *CRE-ER^{T2}*, wild-type and *COUP-TFII $^{F/+}$* embryos. This demonstrates that developmental defects observed in inducible *COUP-TFII* knockout mutants (*CRE-ER^{T2}; COUP-TFII $^{F/F}$*) are due to *COUP-TFII* ablation and not *Cre* toxicity.

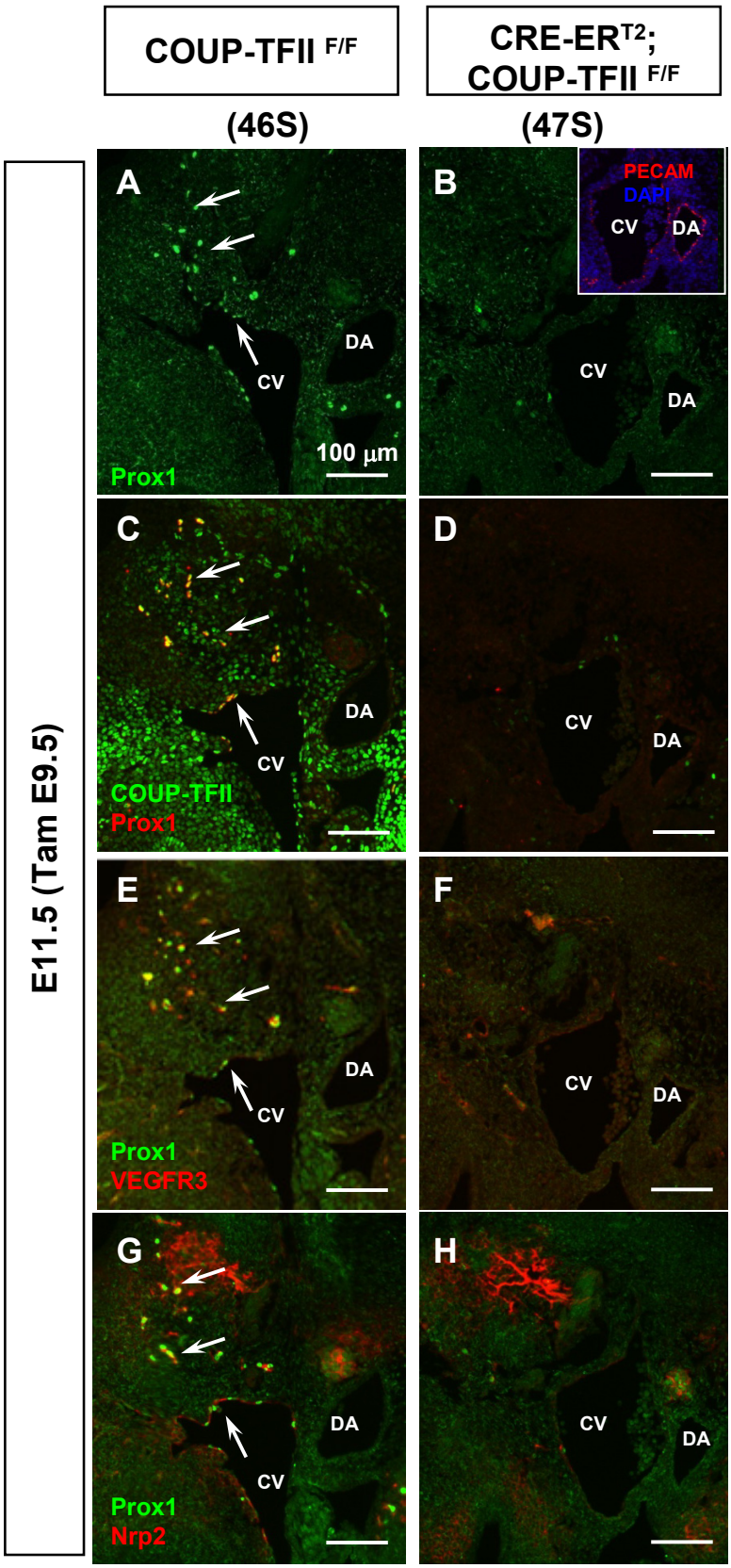

Supplementary Figure 4. Absence of lymphatic endothelial progenitor cells in inducible *COUP-TFII* mutants.

Transverse sections of 46-somite-stage *COUP-TFII* $^{F/F}$ controls and 47-somite-stage *CRE-ER*^{T2}*; COUP-TFII* $^{F/F}$ embryos (administration of Tam at E9.5) were analyzed using antibodies against Prox1 (A-H), COUP-TFII (C, D), VEGFR3 (E, F), and Nrp2 (G, H). (A, C, E, G) Prox1, COUP-TFII, VEGFR3, and Nrp2-expressing LEC progenitors (arrows) were visualized migrating out from one side of the cardinal vein to form the lymphatic sacs. (B, D, F, H) In contrast, the mutant embryos displayed complete absence of LEC progenitors. PECAM staining (red) and DAPI staining (blue) mark endothelium and nuclei, respectively (B, inset). CV, cardinal vein; DA, dorsal aorta. Scale bar, 100 μm.

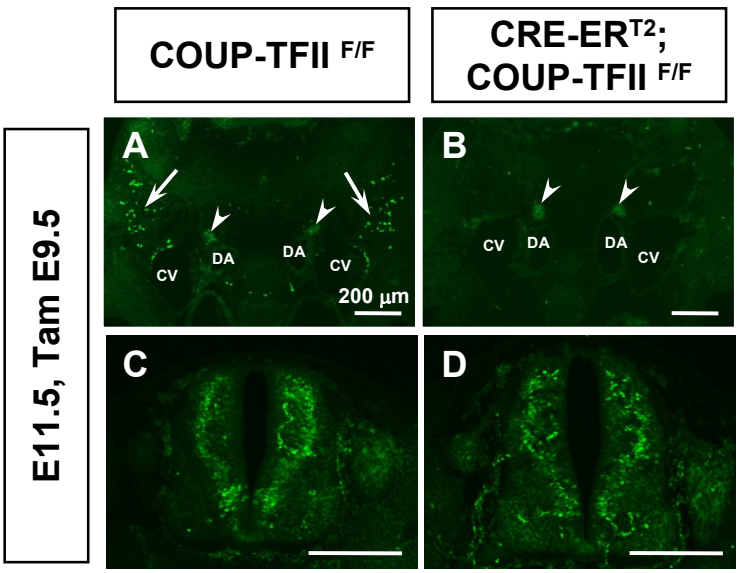

Supplementary Figure 5. Absence of Prox1-positive lymphatic endothelial progenitor cells, but retention of Prox1 expression in the neural tube and the sympathetic ganglia in inducible *COUP-TFII* mutants.

(A-D) Immunofluorescent staining of transverse sections of E11.5 *COUP-TFII* $^{F/F}$ controls and *CRE-ER*^{T2}*; COUP-TFII* $^{F/F}$ embryos (Tam administration at E9.5) with antibodies against Prox1 (green). (A, B) Control embryos exhibited Prox1-positive LECs migrating from the cardinal vein (arrows), whereas inducible *COUP-TFII* mutants showed complete absence of Prox1-positive LECs. In contrast, Prox1 expression was unaffected in the sympathetic ganglia (A, B, arrowheads) and neural tube (C, D) in both control and mutant embryos, indicating that the lack of expression of Prox1 in E11.5 conditional *COUP-TFII* mutants is LEC selective. Scale bar, 200 μm.

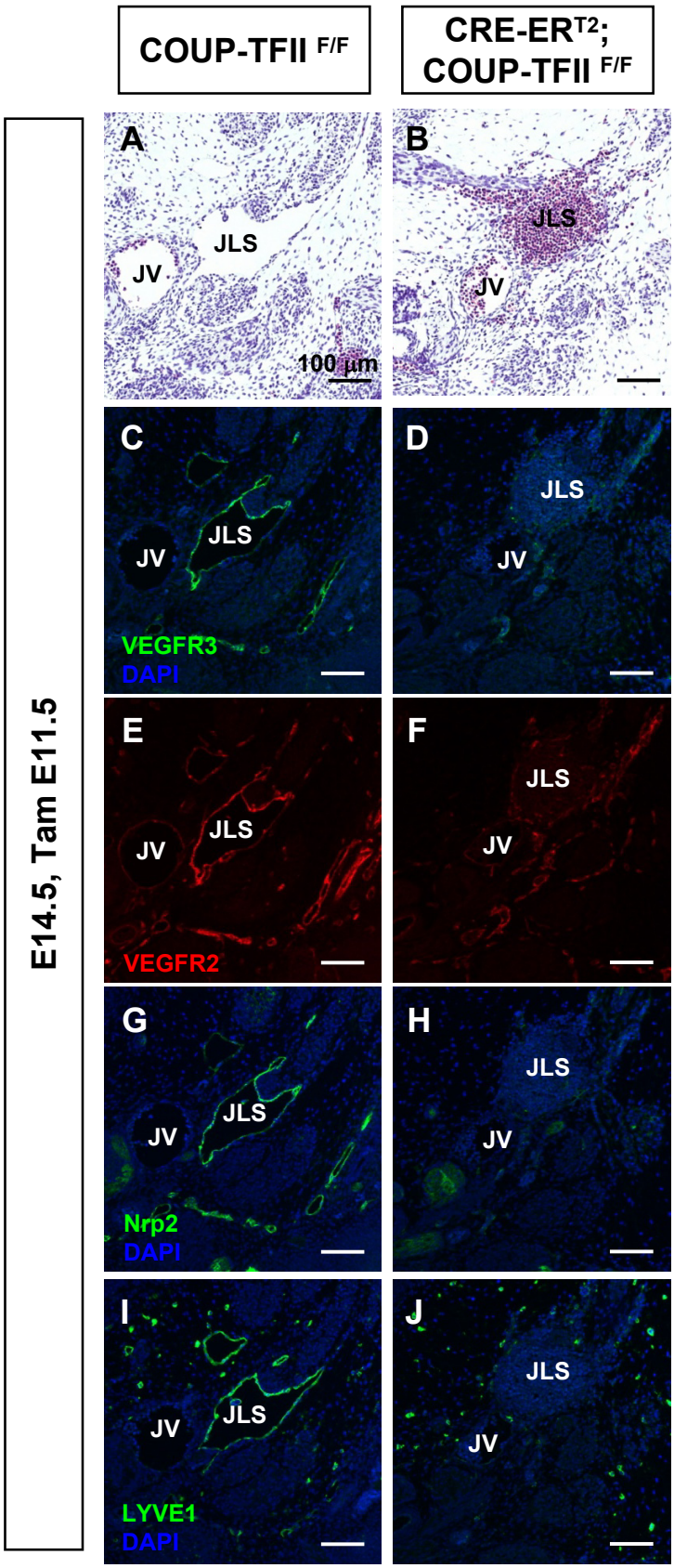

Supplementary Figure 6. Inducible *COUP-TFII* mutants show the malformation of jugular lymphatic sacs. Analysis of transverse sections of *COUP-TFII* $^{F/F}$ controls and *CRE-ER*^{T2}*; COUP-TFII* $^{F/F}$ mutant embryos at E14.5 (administration of Tam at E11.5). (A, B) Sections were stained with H&E. Jugular lymphatic sac (JLS) in the mutant is malformed and filled with blood. (C-F) Immunostaining with markers VEGFR3 (C, D), and VEGFR2 (E, F), and nuclei were counterstained with DAPI. The expression of VEGFR3 and VEGFR2 is high in JLS of controls (C, E), but barely detectable in JLS of mutants (D, F). (G-J) Immunostaining with lymphatic markers, Nrp2 (G, H) and LYVE1 (I, J). Robust expression is detected in controls (G, I), but hardly detectable in mutants (H, J). JLS, jugular lymphatic sac; JV, jugular vein. Scale bar, 100 μm.

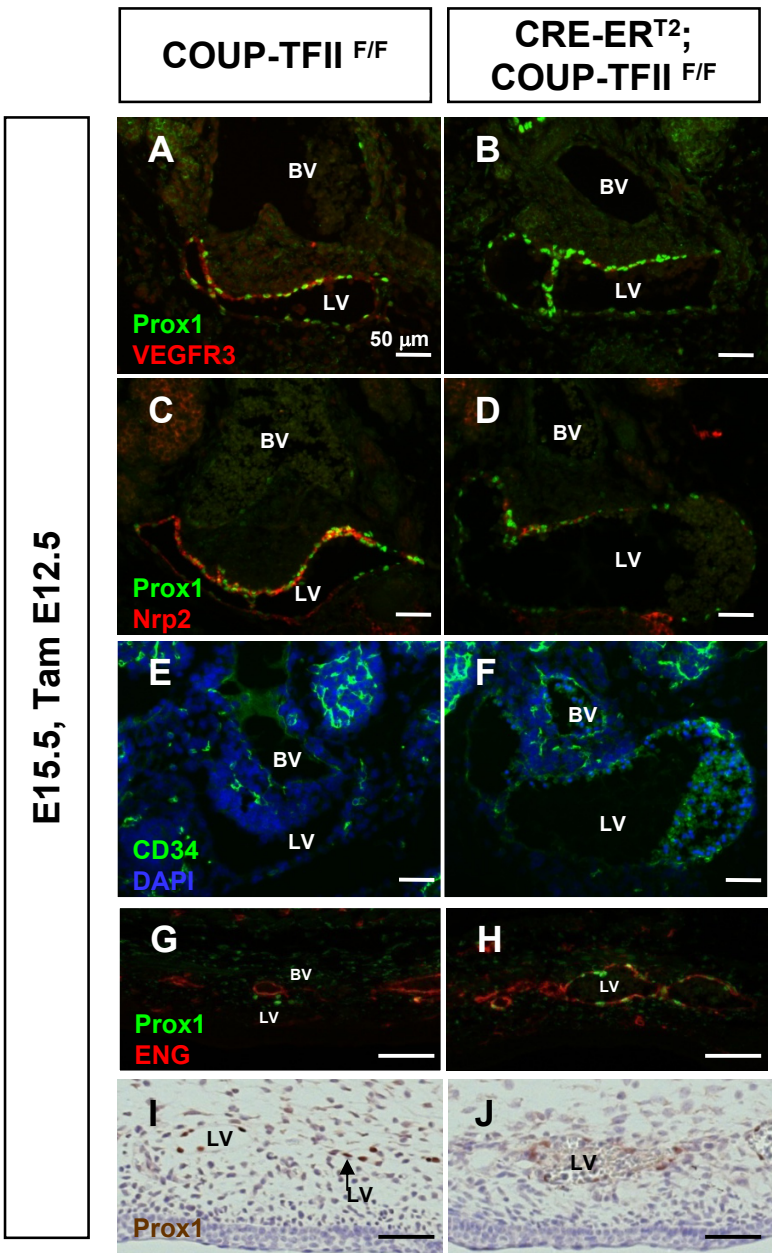

Supplementary Figure 7. Loss of lymphatic identity and gain of blood endothelial cells characteristics in the inducible *COUP-TFII* mutant mice.
Immunofluorescence microscopy of transverse sections of E15.5 controls and *CRE-ER^{T2}; COUP-TFII $^{F/F}$* mutants (administration of Tam at E12.5) using an antibody as marked. (A-H) Down-regulation of VEGFR3 and Nrp2 expression and ectopic expression of CD34 and endoglin were observed in lymphatic vessels (A-F) and in dermal lymphatic vessels (G-H) in the inducible *COUP-TFII* mutants. (I, J) Prox1 immunostaining shows the dilated and blood-filled dermal lymphatic vessels in the E15.5 inducible *COUP-TFII* mutants. BV, blood vessel; LV, lymphatic vessel. Scale bar, 50 µm.

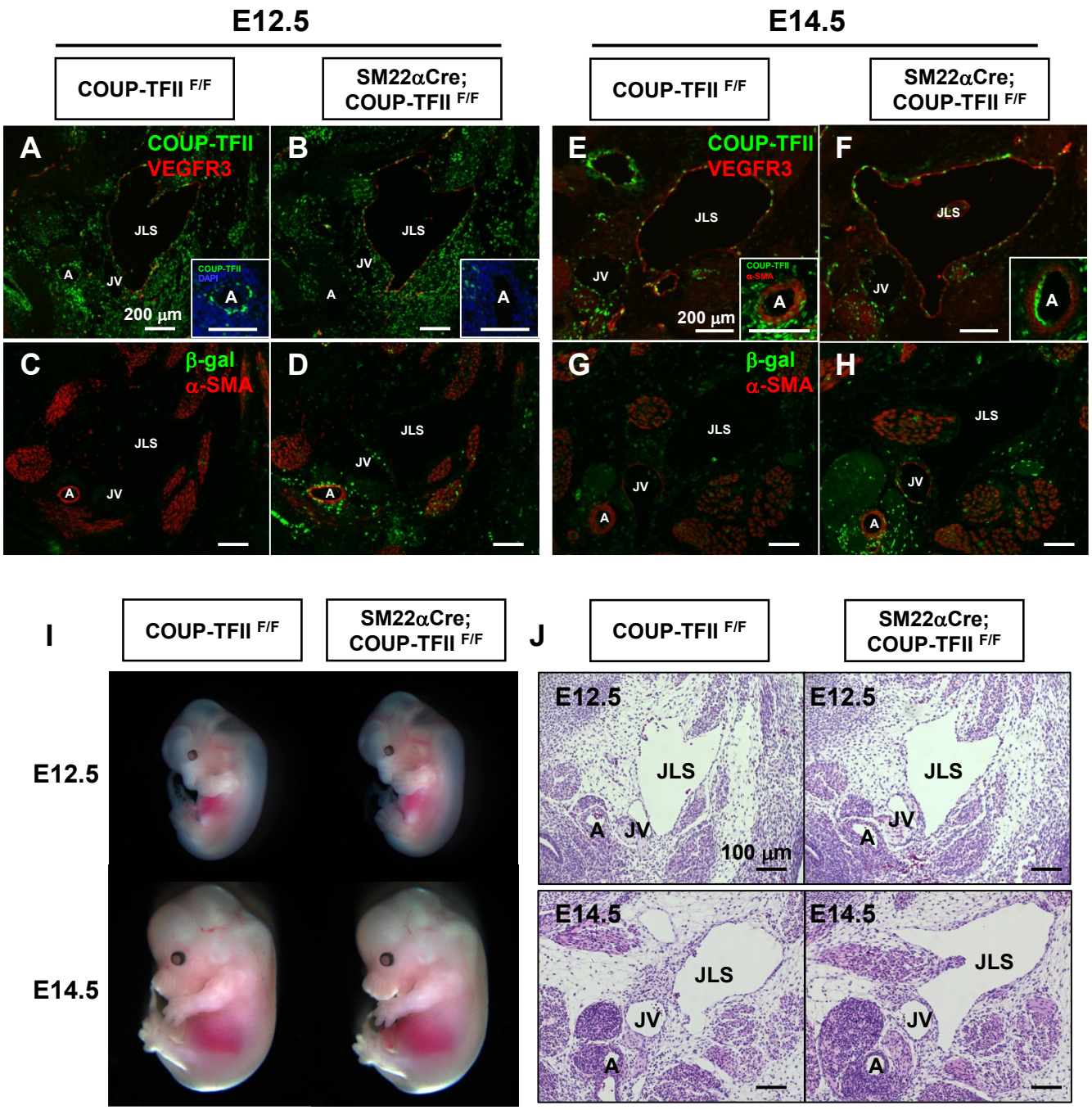

Supplementary Figure 8. Loss of *COUP-TFII* in smooth muscle cells (SMCs) does not have major effects on lymphangiogenesis between E12.5 and E14.5.

(A-H) Immunofluorescent staining of transverse sections of E12.5 (A-D) and E14.5 (E-H) embryos. COUP-TFII (green) was deleted (A versus B, E versus F), and β-gal (green) was expressed (C versus D, G versus H) in the α-SMA (red)-positive SMCs of the artery of *SM22αCre; COUP-TFII*$^{F/F}$ embryos at E12.5 (A-D) and E14.5 (E-H). Insets in A, B, E, and F are higher-magnification images of the COUP-TFII staining (green) in the artery. Endothelial cells of jugular lymphatic sac from control and *SM22αCre; COUP-TFII*$^{F/F}$ embryos expressed VEGFR3 (red) (A versus B, E versus F), indicating normal lymphatic identity in *SM22αCre; COUP-TFII*$^{F/F}$ embryos. (I) Normal macroscopic appearance of E12.5 and E14.5 control and *SM22αCre; COUP-TFII*$^{F/F}$ embryos. (J) H&E stained transverse sections through the jugular region of E12.5 and E14.5 *COUP-TFII*$^{F/F}$ control and *SM22αCre; COUP-TFII*$^{F/F}$ embryos. A, artery; JV, jugular vein; JLS, jugular lymphatic sac. Scale bar, 100 μm.

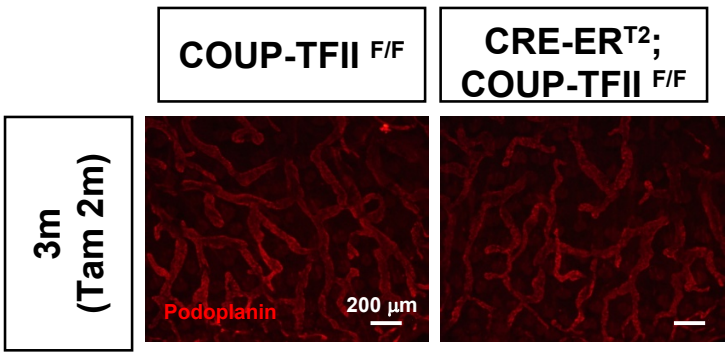

Supplementary Figure 9. Normal lymphatic identity in the inducible *COUP-TFII* mutant mice. Whole-mount immunofluorescent staining for Podoplanin (red) from the ears of 3-month-old *COUP-TFII* $^{F/F}$ control and *CRE-ER*^{T2}*; COUP-TFII* $^{F/F}$ mutant adults (with Tam-mediated COUP-TFII deletion at 2-months old). Scale bar, 200 μm.

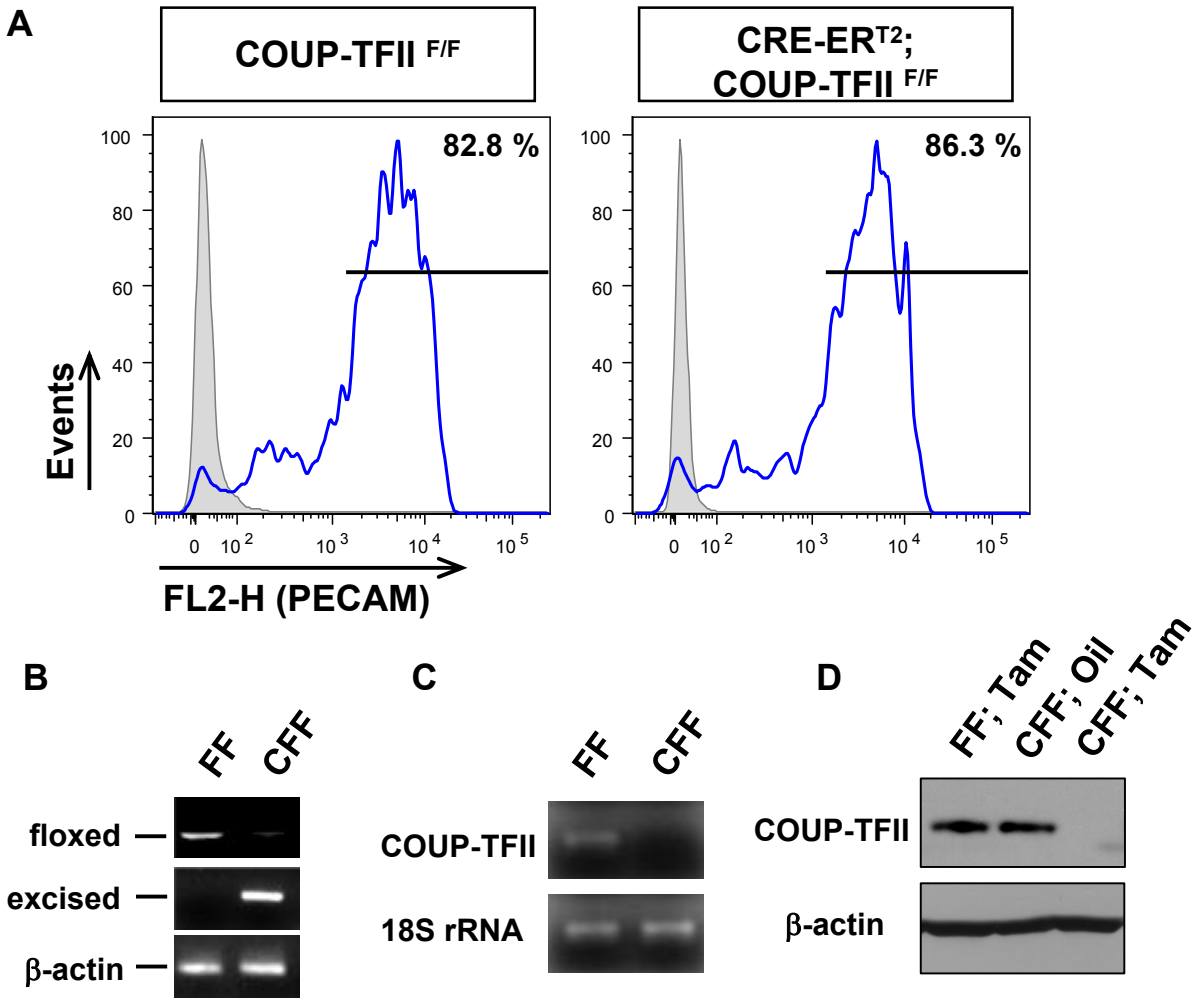

Supplemental Figure 10. Inactivation of *COUP-TFII* in mouse lung ECs.
(A) ECs were isolated from 3-month-old *COUP-TFII* $^{F/F}$ (FF) controls and *CRE-ER*^{T2}*; COUP-TFII* $^{F/F}$ (CFF) adults (with Tam-mediated COUP-TFII deletion at 2-months old). Mouse lungs were digested, stained with PECAM and analyzed by FACS. Gray histograms represent the isotype control. PECAM-gated ECs were sorted. (B) Genomic DNAs were isolated from sorted cells for PCR genotyping and allele excision analysis, and β-actin was used as a loading control. (C) COUP-TFII expression in sorted ECs from *COUP-TFII* $^{F/F}$ and *CRE-ER*^{T2}*; COUP-TFII* $^{F/F}$ adult mice was analyzed by semi-quantitative RT-PCR, and 18S rRNA served as a loading control. (D) Detection of COUP-TFII and β-actin protein levels by western blot of whole lung lysates from 4-month-old FF, CFF (with oil treatment at 2-months old), and CFF (with Tam-mediated COUP-TFII deletion at 2-months old).

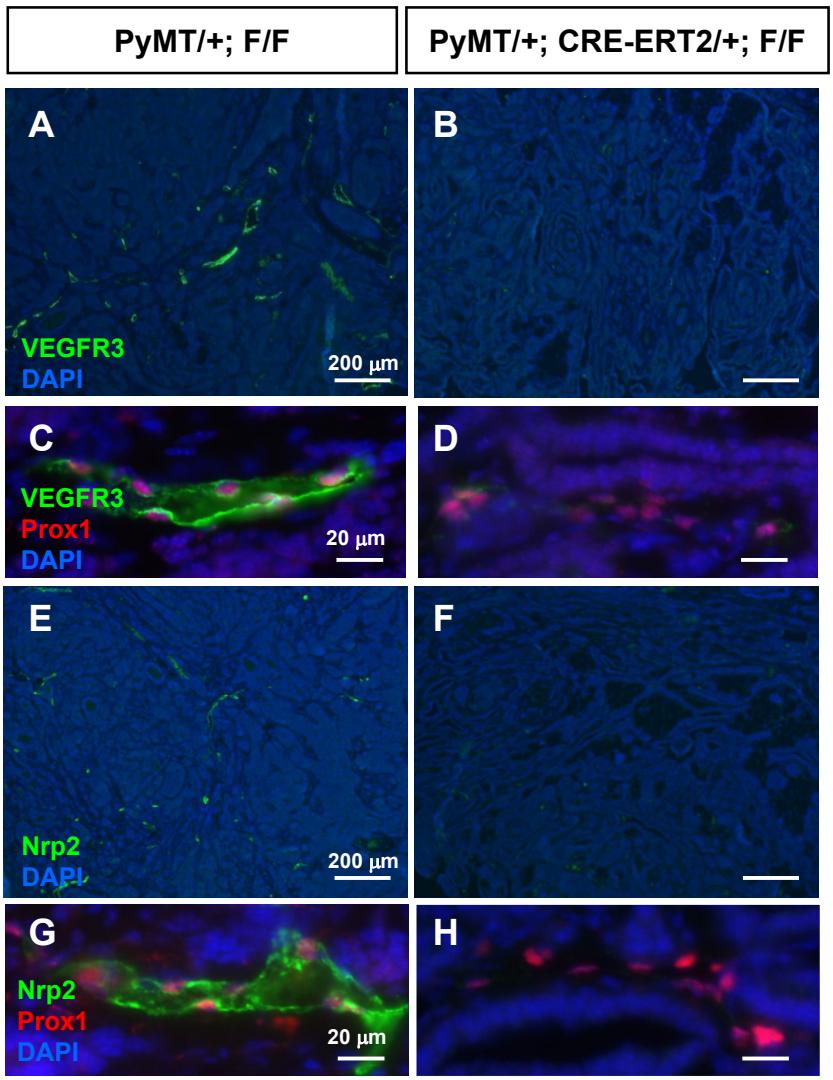

Supplementary Figure 11. The expression of VEGFR3 and Nrp2 is reduced in the tumor lymphatics of adult inducible *COUP-TFII* mutant mice.

Immunofluorescence microscopy of mammary gland tumor sections from *PyMT/+; F/F* controls or *PyMT/+; CRE-ER^{T2}/+; F/F* mutant littermates at 4.5 months old using an antibody against VEGFR3 (green, A-D), Nrp2 (green, E-H), and Prox1 (red, C, D, G, H). Nuclei were counterstained with DAPI. The expression of VEGFR3 and Nrp2 is reduced in Prox1-positive tumor lymphatics in mutants (B, D, F, H) versus controls (A, C, E, G). Scale bar, 200 µm in (A, B, E, F); 20 µm in (C, D, G, H).

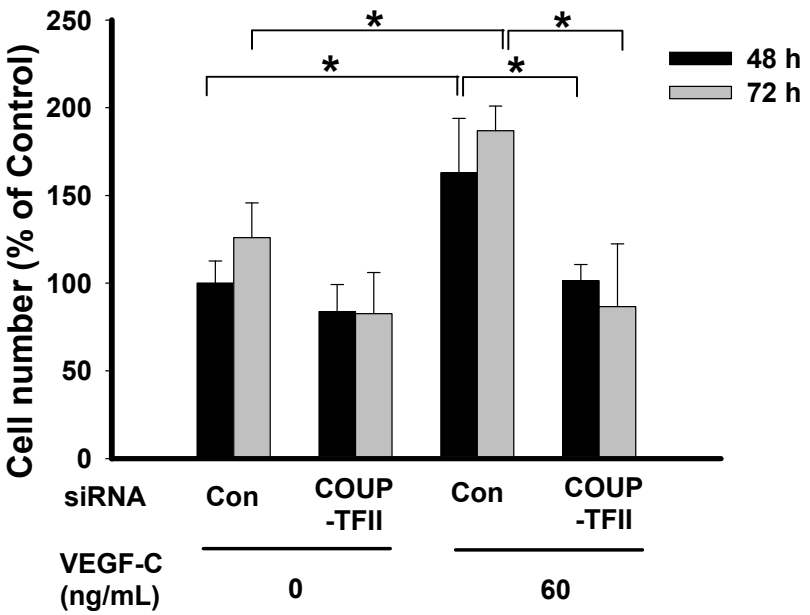

Supplementary Figure 12. Knock down of *COUP-TFII* inhibits lymphatic endothelial cell proliferation in the presence of VEGF-C.

Human primary LECs were transfected with scrambled or *COUP-TFII* siRNA for 48 hours. Cells were re-plated and cultured in medium without serum for 12 hours and subsequently incubated in the presence of VEGF-C for 48 or 72 hours. Cell numbers were quantified at the indicated time points. Error bars indicate standard deviation; **P*<0.05

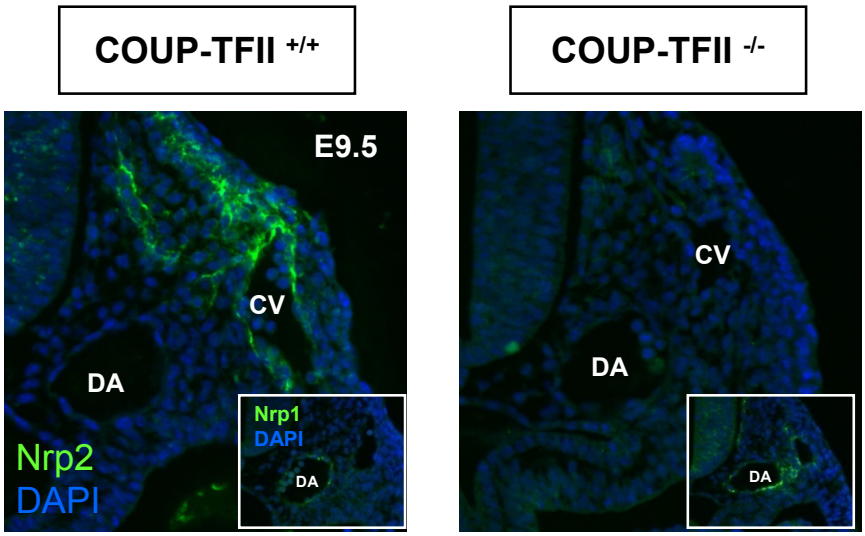

Supplementary Figure 13. Nrp2 expression is reduced in the cardinal vein of E9.5 *COUP-TFII* null mutants.
Immunofluorescence for Nrp2 and Nrp1 (inset) in transverse sections of E9.5 wild type and *COUP-TFII*$^{-/-}$ embryos. Nrp2 and Nrp1 are expressed in the cardinal vein and dorsal aorta of the wild type, respectively. In contrast, Nrp2 expression is reduced in the cardinal veins, whereas Nrp1 is ectopically expressed in the dorsal aorta of E9.5 *COUP-TFII* null embryos. Nuclei were counterstained with DAPI. CV, cardinal vein; DA, dorsal aorta.

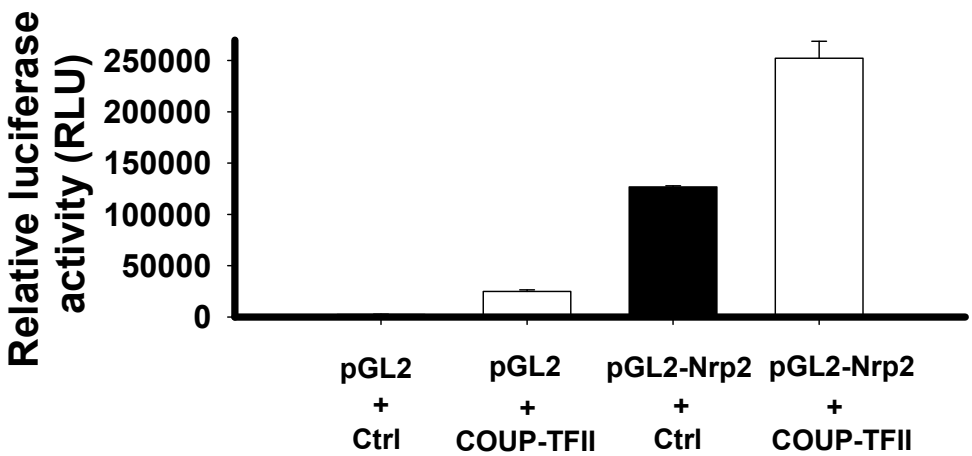

Supplementary Figure 14. COUP-TFII binds to *Nrp2* promoter and activates its transcription.
HEK293T cells were transiently transfected with the Nrp2 promoter-luciferase reporter (pGL2-NP2) and an empty control vector (pGL2) with a control vector (Ctrl) or a COUP-TFII-expressing vector (COUP-TFII). The results are expressed as relative luciferase activity after correction for β-gal activity. COUP-TFII enhances *Nrp2* transcriptional activity. Error bars represent standard deviation.

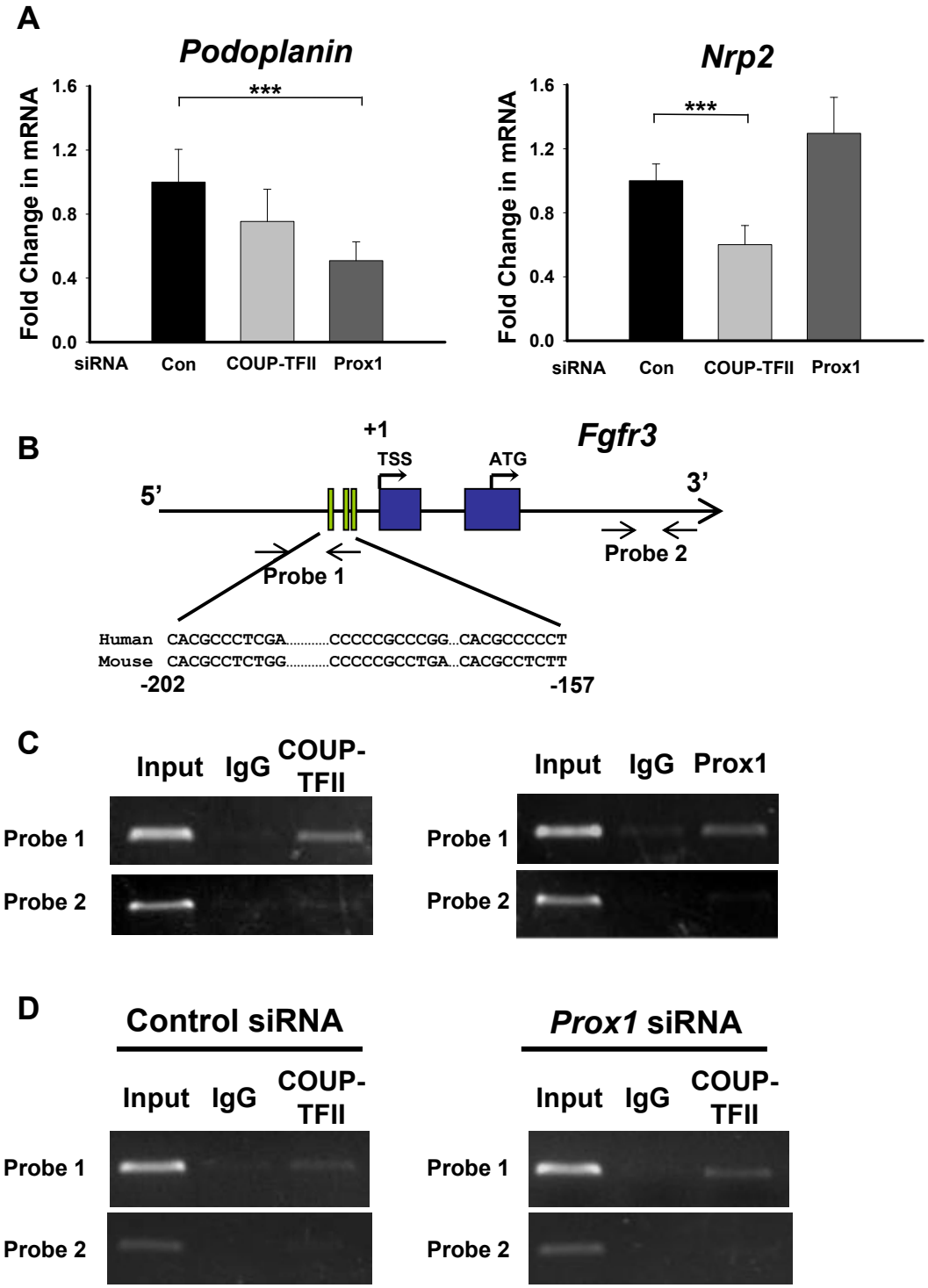

Supplementary Figure 15. ChIP analysis of COUP-TFII and Prox1 binding to the human genomic *FGFR3* promoter in human primary LECs.

(A) Quantitative RT-PCR analysis of lymphatic-specific transcripts in RNA isolated from scrambled, *COUP-TFII* or *Prox1* siRNA transfected human primary LECs (normalization to 18S rRNA). Error bars indicate standard deviation; ***P<0.01. (B) The sequences and positions of the three putative Prox1-binding sites found in the *FGFR3* promoter are indicated (7). TSS, transcription start site. (C, D) Human primary LECs were transfected with scrambled siRNA (C, and D, left panel) or *Prox1* siRNA (D, right panel). After 72 hours, chromatin-bound DNA was immunoprecipitated with antibodies against COUP-TFII, Prox1, or IgG control. Immunoprecipitated DNA was analyzed by PCR. (C) ChIP analysis shows recruitment of COUP-TFII and Prox1 to regions containing the putative Prox1-binding sites of human *FGFR3* promoter in LECs transfected with scrambled siRNA. (D) Knocking down of *Prox1* did not affect the recruitment of COUP-TFII on the *FGFR3* promoter.

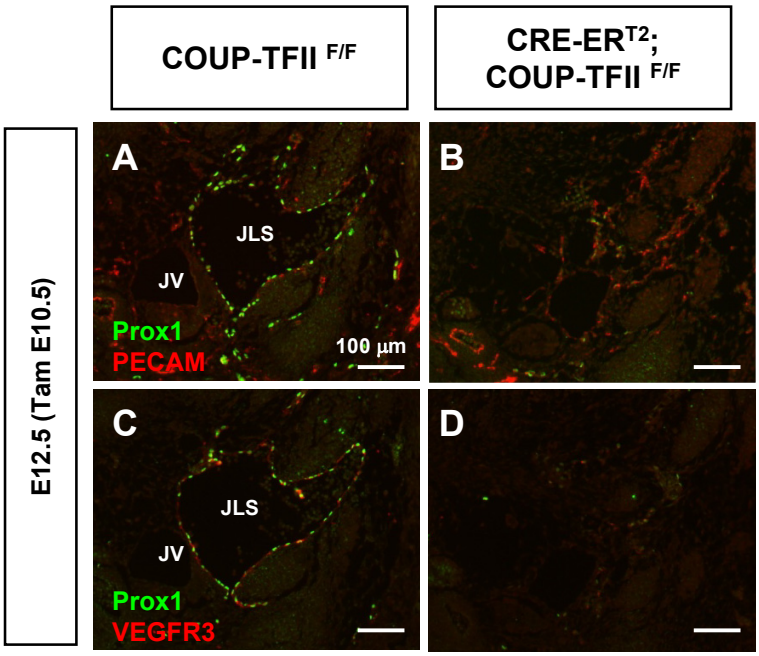

Supplementary Figure 16. ***COUP-TFII*** **is required for the LEC differentiation and the initial formation of lymphatic sacs.**
Immunofluorescent images of transverse sections of control *COUP-TFII* $^{F/F}$ and littermate *CRE-ER*^{T2}*; COUP-TFII* $^{F/F}$ mutant embryos at E12.5 (with Tam administration at E10.5). When COUP-TFII excision was induced at E10.5, PECAM positive endothelial cells (red) are seen in controls (A) and mutants (B). However, very low levels of Prox1 (B) and VEGFR3 (D) are detected in mutants in comparison to robust expression in controls (A, C) at E12.5. Scale bar, 100 μm.